Electronic Supplementary Information (ESI) for Chemical Communications

Two-step resonance-energy-transfer-based ratiometric biosensor for sensing and annihilation of *Staphylococcus aureus*

Qiumei Feng[a], Tao Wu[a], Huan Wang[a], Meisheng Wu[b,*], Baoting Dou[a], and Po Wang[a,*]

[a] *School of Chemistry and Materials Science, Jiangsu Normal University, Xuzhou 221116, China*

[b] *Department of Chemistry, College of Science, Nanjing Agricultural University, Nanjing 210095, China*

E-mail: wumeisheng@njau.edu.cn (M. Wu); wangpo@jsnu.edu.cn (P. Wang).

Note added after publication: This supplementary information file replaces the version that was published on 30th January 2024. Figure S9, the text on page S12 from "Besides, the fabrication reproducibility" onwards, and the author contribution statement have been added.

Experimental Section

Materials: Sodium sulfide ($Na_2S \cdot 9H_2O$), 2-aminoethanethiol, cadmium nitrate tetrahydrate ($Cd(NO_3)_2 \cdot 4H_2O$), vancomycin hydrochloride (Van), tetrachloroaurate hydrate ($HAuCl_4 \cdot 4H_2O$) and potassium peroxydisulfate ($K_2S_2O_8$) were purchased from Sinopharm Chemical Reagent Co. Ltd (Shanghai, China). Sodium borohydride ($NaBH_4$), tris (2-carboxyethyl) phosphine hydrochloride (TCEP), N-(3-dimethylaminopropyl)-N-ethyl-carbodiimide hydrochloride (EDC), 6-mercapto-1-hexanol (MCH), bovine serum albumin (BSA) and N-hydroxysuccinimide (NHS) were bought from Sigma-Aldrich (U.S.A). Carboxylated magnetic beads (20 nm in diameter) were obtained from Xi'an GoldMag Nanobiotech Co., Ltd (Xi'an, China). All pathogenic bacteria including *Listeria monocytogenes* (*L. monocytogenes*, ATCC 19115), *Salmonella typhimurium* (*S. typhimurium*, ATCC 14028), *Bacillus subtilis* (*B. subtilis*, CCTCCAB 90008), *Escherichia coli* (*E. coli*, ATCC25922), and *Staphylococcus aureus* (*S. aureus*, ATCC 29213) were supplied by Guangdong Institute of Microbiology (Guangzhou, China). The mixture of 0.1 M KH_2PO_4 and 0.1 M K_2HPO_4 was applied for the preparation of phosphate buffered solution (PBS, pH 7.4). All oligonucleotides were synthesized by Sangon Biological Engineering Technology & Services Co. Ltd. (Shanghai, China) and the corresponding DNA sequences were shown in Table S1.

Apparatus: A MPI-A multifunctional electrochemical and chemiluminescent analytical system with 350-800 nm spectral width of photomultiplier tube (PMT) were applied to record all the ECL emission measurements. A conventional three-electrode cell consisting of a Pt wire as counter electrode, Ag/AgCl electrode as reference electrode, and the modified glassy carbon electrode (GCE) (3 mm in diameter) as working electrode was applied for all experiments. Electrochemical impedance spectroscopy (EIS) tests were monitored by a CHI 660E electrochemical workstation with the following experimental conditions: DC potential, 0.22 V; frequency range, $10^5-0.1$ Hz; and amplitude, 0.005 V. Fluorescence spectra were recorded on an RF-5301PC fluorescence spectrometer (Shimadzu Co., Japan). UV−vis absorption spectra were recorded on a UV-

3600 UV−vis−NIR spectrophotometer (Shimadzu Co. Kyoto, Japan). Transmission electron micrograph (TEM) images of CdS QDs and Au NPs were collected from a JSM-2100 Plus (JEC, Japan). The morphology of *S. aureus* was characterized by scanning electron microscopy (SEM, JSM-6330F microanalyzer, JEOL, Japan). X-ray photoelectron spectroscopy (XPS) data were obtained on a Thermo ESCALAB 250XI instrument with Al Kα X-ray source (Thermo Fisher Scientific Inc., U.K.). X-ray diffraction (XRD) measurement was performed on a D/MAX 2200 VPC diffractometer using Cu Kα radiation ($\lambda = 0.154056$ nm) with a Ni filter (Rigaku, Japan).

Synthesis of CdS QDs: CdS QDs were synthesized according to previous literatures.[S1,S2] Briefly, $Cd(NO_3)_2 \cdot 4H_2O$ (0.1861 g) was homogeneously dissolved in ultrapure water (30 mL), followed by reacting for 30 min at 70 °C under vigorous stirring. Subsequently, 30 mL of freshly prepared Na_2S solution (0.083 M) was injected into the above solution and refluxed for 3 h at 70 °C. The resulting orange-yellow precipitates were centrifuged at 8000 rpm for 8 min and washed with ethanol and water. The purified precipitates were ultrasonically dispersed into ultrapure water and then centrifuged at 9000 rpm for 10 min to collect the upper yellow solution.

Preparation of W-Van: First, 1 mL of vancomycin hydrochloride (Van, 1% w/v) was treated by a mixture of 10 mg/mL NHS and 20 mg/mL EDC at 30 °C for 1 h. Then, 69 µL of W strands was mixed with the activated Van solution, incubating at 30 °C for 24 h. After purification, the prepared W-Van was kept at 4 °C before use.

Preparation of S-Au NPs: Briefly, $NaBH_4$ (0.1 M) was first prepared with cold water and then 0.6 mL of $NaBH_4$ added to 20 mL of $HAuCl_4$ solution (0.25 mM). After stirring for 10 min, the color of solution immediately turned to deep purple-red color, indicating the generation of Au NPs. Then, a volume of 10 µL S strands (100 µM) was introduced into 1 mL of Au NPs solution, stirring for overnight. Before using, 5′ SH-modified S strands were treated by 10 mM TCEP to cleave S−S bonds and further purified by Millipore. Afterward, 2 M NaCl (prepared by PBS) was added to the above solution

stepwise to stabilize the obtained S-Au NPs. Finally, it was centrifuged and rinsed with PBS, then redispersed in PBS.

Bacteria culture and counting: All pathogenic bacteria including *S. aureus*, *L. monocytogenes*, *S. typhimurium*, *B. subtilis* and *E. coli* were cultured in Luria-Bertani broth medium, and maintained in a 37 °C shaking incubator for 24 h. Fresh pathogenic bacteria in PBS were obtained by washing with PBS and centrifugation. Following a serial dilution and incubation on agar plates, the number of pathogenic bacteria with colony forming units per milliliter (CFU/mL) was determined by the agar plate-counting method.

Preparation of FL/ECL biosensor: The fabrication process of the biosensor consisted of dual recognition-triggered target conversion on magnetic beads surface and CHA signal amplification on a modified electrode. First, carboxylated magnetic beads were reacted with the mixture of EDC and NHS in order to active carboxyl groups, and then added into aptamer solution (2.5 μM) labeled with amino groups. After reacting at 37 °C for 1 h, 2.0 wt% bovine serum albumin was applied for blocking the unreacted activated sites of magnetic beads surface. Various concentrations of *S. aureus* and W-Van:M duplex were orderly introduced into aptamer/magnetic beads solution and reacted for 1 h. Here, W-Van:M duplex represented the hybridization product of W-Van and M strands. Subsequently, excess W-Van:M duplex was removed by magnetic separation, and the resultant W-Van:M/*S. aureus*/aptamer/magnetic beads further underwent the treatment of H1 strands. Followed by purifying, H1/W-Van:M/*S. aureus*/aptamer/magnetic beads were obtained as dual recognition-triggered target conversion.

Besides, a glassy carbon electrode (GCE) was treated with alumina slurries to obtain the mirror-like GCE surface. 10 μL of CdS QDs were dropped onto GCE surface. After drying, the loose bounded CdS QDs on GCE surface were removed by immersing in phosphate buffered solution (PBS). Subsequently, the resultant CdS QDs/GCE was dipped into 2.0 μM stem-loop structured H2 for overnight at 4 °C to form H2/CdS QDs/GCE via Cd-S bond. Prior to use, H2 was activated by TCEP to cut S−S bonds.

After that, the resulting electrode was transferred into 100 µM 6-mercapto-1-hexanol solution for 1 h to block the surface. Next, H2/CdS QDs/GCE was incubated with the as-prepared H1/W-Van:M/*S. aureus*/aptamer/magnetic beads and the enzyme-free signal amplification on the electrode interface was activated. After reacting for 60 min, the obtained H1/H2/CdS QDs/GCE was further incubated with S-Au NPs:P-FAM duplex for 50 min, forming S-Au NPs/H1/H2/CdS QDs/GCE. S-Au NPs:P-FAM duplex was the hybrid product of S-Au NPs and P-FAM.

Assay Procedure: Following incubating, the constructed electrode interface was placed in 0.05 M $K_2S_2O_8$ (prepared by 0.1 M PBS, pH 8.3) for ECL measurements. During the detection, a cyclic potential range from 0 to –1.2 V and 600 V of photomultiplier tube were applied. The scan rate was set at 100 mV/s. In addition, the FL spectra of the remaining supernatant were measured at an excitation wavelength of 490 nm.

Native polyacrylamide gel electrophoresis (PAGE) analysis: In order to confirm the feasibility of aptamer to *S. aureus* recognition and enzyme-free CHA signal amplification on electrode interface, PAGE-based analysis was performed as follows: DNA samples and ladder DNA solution as indicator were first mixed with 6×loading buffer with a volume ratio of 5:1, and then loaded into 16% PAGE, followed by running in 1×TBE buffer (pH 8.0) for 120 min at 100 V. PAGE was finally stained with ethidium bromide and taken a picture using the Bio-Rad imaging system (Hercules, CA, U.S.A.).

Detection of *S. aureus* in real samples: The designed biosensor was used for the detection of *S. aureus* in food samples. Egg, meat paste and raw milk samples were obtained from local stores and pretreated according to our previous work.[S3] Then, *S. aureus* was added at the known concentration to 100-fold diluted egg white and meat paste, and 10-fold diluted raw milk to evaluate the applicability of the proposed method in real samples.

Supplementary Tables and Figures

Table S1. Oligonucleotide sequences used in this work.

| Name	Sequences (5′ to 3′)
Aptamer	NH$_2$-GCAATGGTACGGTACTTCCTCGGCACGTTCTCAGTAGCGCTCG CTGGTCATCCCACAGCTACGTCAAAAGTGCACGCTACTTTGCTAA
W	NH$_2$-ATAAGGCACGACGGCAGATGTCGTCTACACATGGC
M	GCCGTCGTGCCTTATTTTTT
H1	GTCAGTGATCGTCTACACATTTACCGGATGTCGCCATGTGTAGACGA CATCT
H2	AGATGTCGTCTACACATGGCGACATCGGTAACCTAGCCCATGTGTA GACAGTCGATGGCTA-SH
S	SH-TAGCCATCGACTGTCTACACA
P	CAGTCGATGGCTTTTTTT-FAM
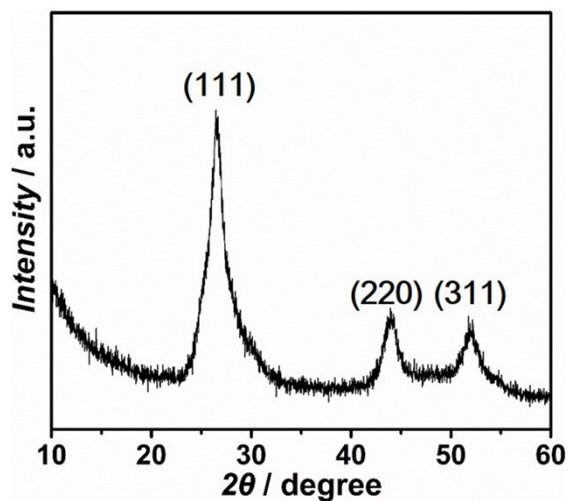
Fig. S1 XRD pattern of CdS QDs.
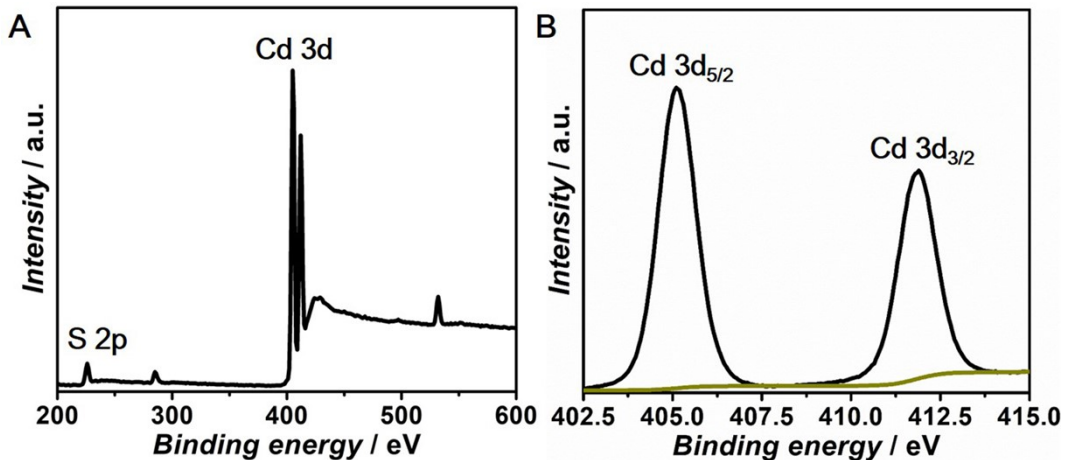
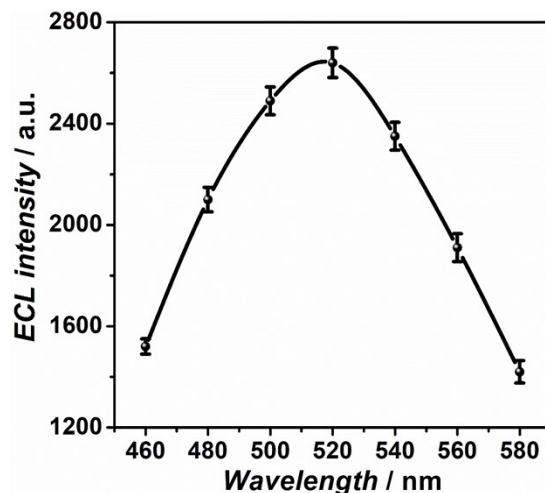**Fig. S2** (A) XPS survey spectrum of CdS QDs. (B) The high-resolution XPS spectrum of Cd 3d region.

Fig. S3 ECL spectrum intensities of CdS QDs obtained using a series of optical filters (460, 480, 500, 520, 540, 560 and 580 nm).

In addition, to further inspect the desired reactions initiated by the designed DNA sequences, UV-vis absorption spectra were performed. Curve a in Fig. S4A showed that the absorbance of aptamer (2 μM) at 260 nm was 0.180 a.u. Followed by treatment with magnetic beads, the absorbance decreased remarkably to 0.013 a.u. (curve b), suggesting that aptamer was modified on magnetic bead surface. Curve c (0.132 a.u.), curve d (0.296 a.u.) and curve e (0.358 a.u.) were the UV–vis spectra of M, W-Van and W-Van:M duplex. These increasing values indicated the successful label of Van at the end of W

strands and the formation of W-Van:M duplex. With the further addition of *S. aureus* and aptamer/magnetic into W-Van:M duplex and then magnetic separation, the absorbance of the supernatant exhibited a sharp decrement (curve f, 0.032 a.u.), implying the feasibility of Van and aptamer for simultaneous binding of *S. aureus*. Upon H1 addition, the absorption peak of the supernatant (curve h, 0.047 a.u.) was reduced markedly in comparison of that of H1 (curve g, 0.160 a.u.), indicating the hybridization between W-Van and H1. Fig. S4B exhibited UV–vis responses of oligonucleotide assembly on electrode surface. Curve a was the absorbance spectrum of 2 μM H2 (0.137 a.u.). The absorption peak at 260 nm decreased markedly after incubation with CdS QDs/GCE (curve b, 0.038 a.u.), attributing to the immobilization of H2 on CdS QDs surface. Similar to H2 (curve a), S:P duplex also exhibited a strong absorbance peak (curve c, 0.192 a.u.). After the treatment of H1/H2/CdS QDs/GCE, the intensity of peak decreased to 0.192 a.u. (curve c), confirming the assembly of S on the modified electrode. The above UV–vis results both confirmed the feasibility of the desired DNA assembly.
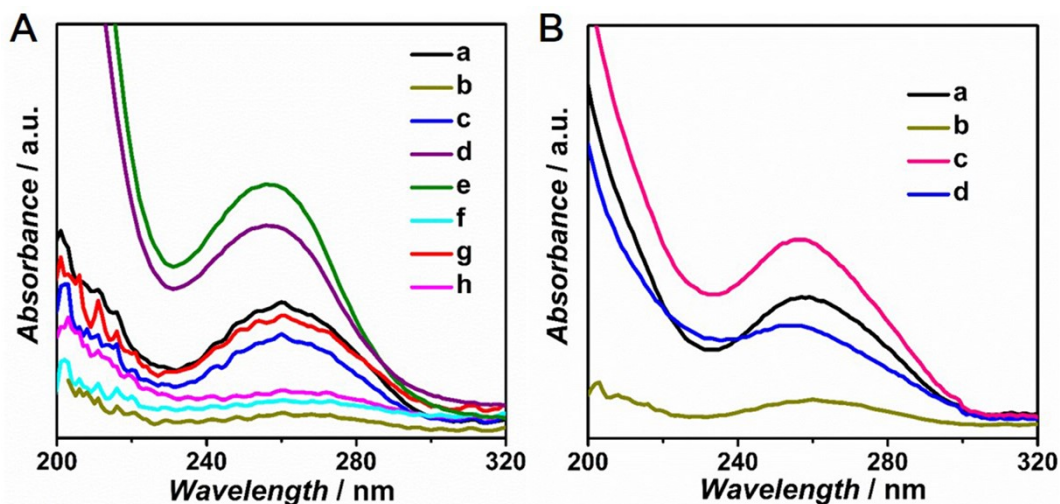

Fig. S4 (A) UV–vis spectra of (a) 2 μM aptamer, (b) supernatant (aptamer + magnetic beads), (c) 2 μM M, (d) W-Van, (e) W-Van:M, (f) supernatant (W-Van:M + *S. aureus* + aptamer/magnetic beads), (g) 2 μM H1, (h) supernatant (W-Van:M/*S. aureus*/aptamer/magnetic beads + H1). (B) UV–vis spectra of (a) 2 μM H2, (b) H2 after incubating with CdS QDs/GCE, (c) S:P, (d) S:P after incubation with H1/H2/CdS QDs/GCE.

Inspired by FRET between fluorescent dyes and Au NPs, P-FAM was selected as the FRET donor and S-Au NPs acted as acceptor to further verify the DNA assembly (Fig. S5). Compared with P-FAM (curve a, 2335 a.u.), the FL spectrum of S-Au NPs:P-FAM duplex exhibited a low intensity (curve b, 369 a.u.) at 527 nm. As a result of FRET, the FL of FAM was inhibited by Au NPs at a very close distance (FL off). Afterward, the S-Au NPs:P-FAM duplex could react with H1/H2/CdS QDs/GCE, and then P-FAM was far from Au NPs, performing the recovery of FL signal (curve c, 1611 a.u.). Taken together, these characterizations of EIS, ECL and FL responses for each fabrication step thus revealed the effectiveness of this design.
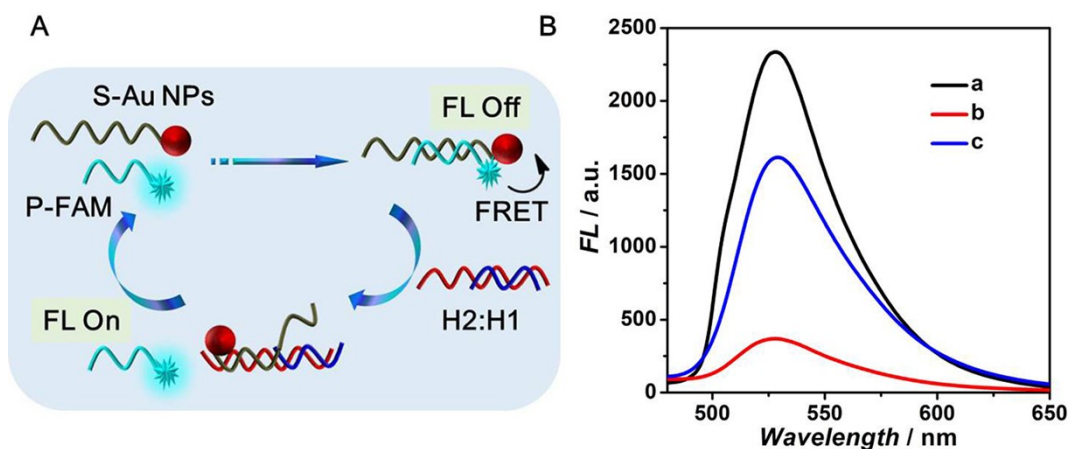

Fig. S5 (A) Mechanism illustration of FRET between S-Au NPs and P-FAM. (B) FL spectra of (a) P-FAM, (b) S-Au NPs:P-FAM, and (c) b incubating with H1/H2/CdS QDs/GCE.

In order to improve the detection performance of the sensor, the experimental conditions including the concentration of H2, the reaction time of CHA and the incubating time between H1/H2/CdS QDs/GCE and S-Au NPs:P-FAM were investigated. As depicted in Fig. S6, the ECL intensity decreased to a minimum value at a H2 concentration of 2.0 μM and increased thereafter with further elevating H2 concentration from 2.5 to 3.0 μM. It was evident that the steric effect of high density H2 on electrode surface may inhibit the subsequent hybridization process. Similarly, Fig. S7 displayed the decrease trend of ECL responses attaching to the reaction time of CHA on electrode interface. With the increase of the reaction time, the hairpin structure of more H2 strands

was opened and then more S-Au NPs were introduced, leading to the quenching of ECL emission from CdS QDs. Thus, the ECL signal decreased and tended to be a constant value at 60 min, displaying that CHA reached the maximum response. Meanwhile, when the incubating time between H1/H2/CdS QDs/GCE and S-Au NPs:P-FAM enhanced, the ratio between FL response and ECL emission (FL/ECL) researched a plateau at 50 min (Fig. S8). After analysis of the experiment results, 2.0 µM of H2 concentration, 60 min of the reaction time for CHA, and 50 min of the incubating time between H1/H2/CdS QDs/GCE and S-Au NPs:P-FAM were selected for subsequent measurements.
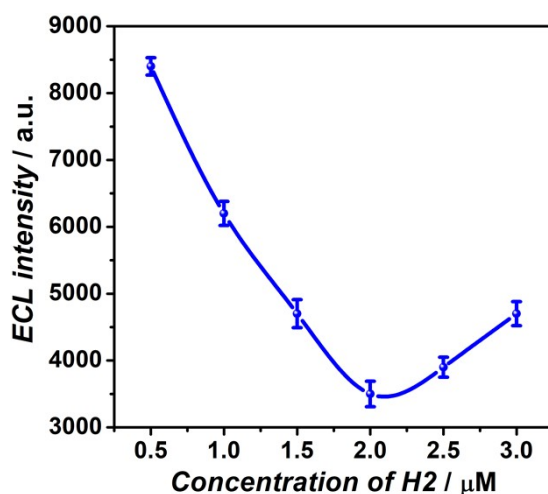

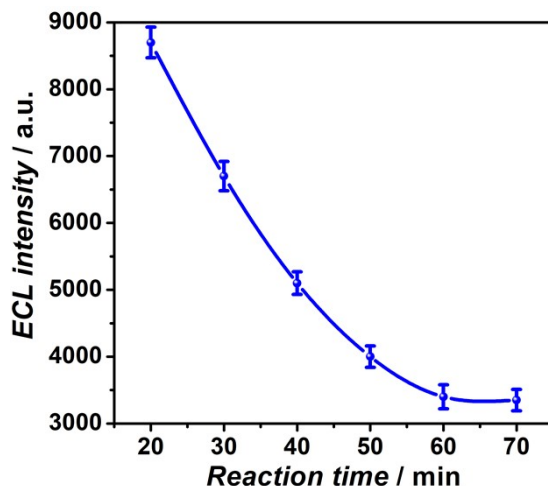**Fig. S6** Influence of H2 concentration on ECL responses toward 10^6 CFU/mL *S. aureus*.

Fig. S7 Effect of the reaction time for catalytic hairpin assembly on ECL responses toward 10^6 CFU/mL *S. aureus*.
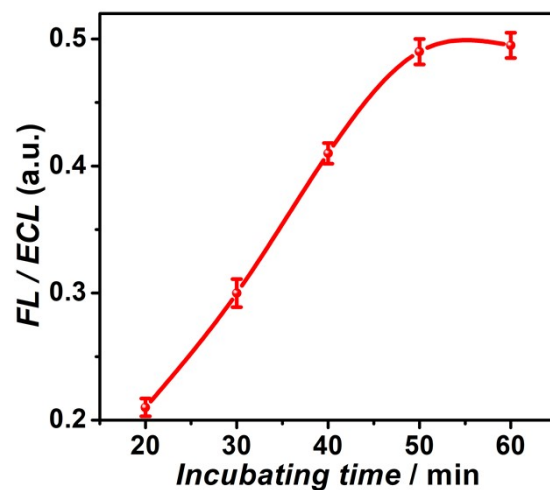
Fig. S8 Effect of the incubating time between H1/H2/CdS QDs/GCE and S-Au NPs:P-FAM on the detection performance of the sensing system. The concentration of *S. aureus* was 10^6 CFU/mL.
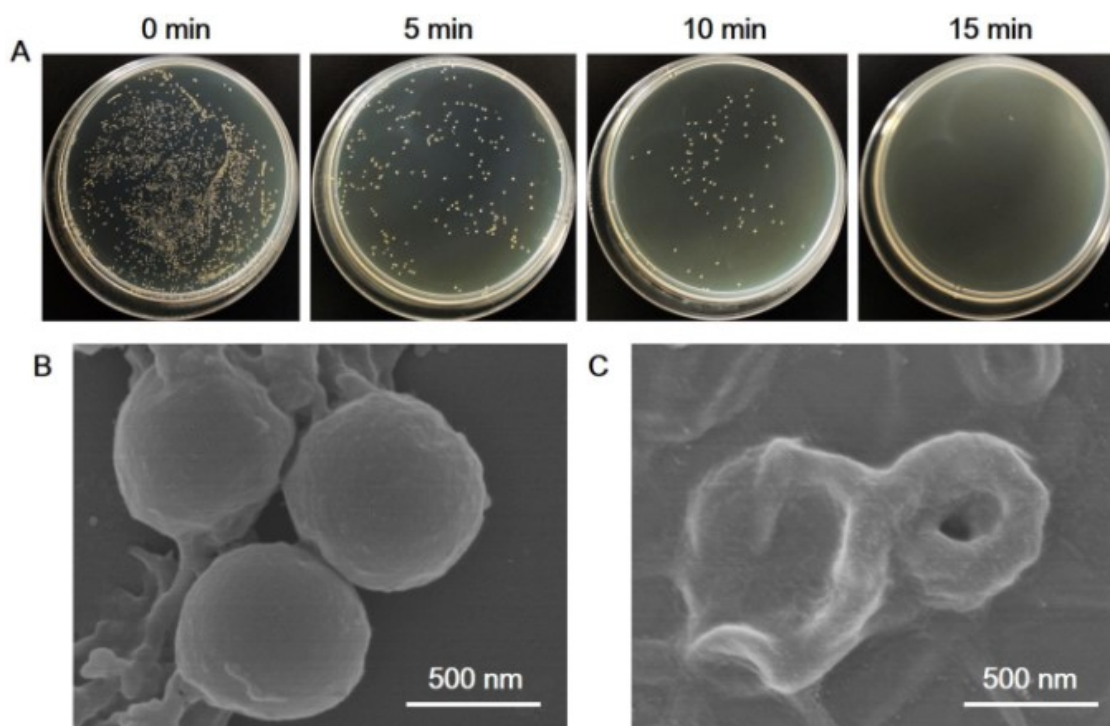

Fig. S9 (A) Photographs of bacterial colonies formed by *S. aureus* after 0, 5, 10, 15 min of exposure to W-Van. SEM images of *S. aureus* without (B) and with (B) the treatment of W-Van.

Table S2. Comparison of different methods for pathogenic bacteria assays.

Methods	Signal amplification strategies	Linear range (CFU/mL)	LOD (CFU/mL)	Ref.
SERS	Gold coated silver decorated graphene oxide	$10-10^6$	10	S4
SERS	Gold nanobones	$10-10^4$	3	S5
Electrochemistry	polyMn-MOF nanosheets	$10-10^8$	1.5	S6
Fluorescence	Two-Step isothermal amplification and metal-organic framework	$130-6.5\times10^4$	40	S7
Fluorescence	Mesoporous silica -modified upconversion	$63-6.3\times10^6$	25	S8
Dynamic light scattering	Gold nanoflowers	$6-6\times10^4$	2.7	S9
Fluorescence	Bidirectional primers exchange reaction cascades	$10-10^5$	9.3	S10
ECL	Cascade signal amplification of CRISPR/Cas12a and primer exchange reaction	$10-10^6$	19	S11
Ratiometric FL/ECL	Dual RET and CHA	$5-10^8$	1	This work

As *S. aureus* was commonly distributed in foods and often caused various foodborne diseases under uncontrolled conditions, the practicability of the sensing platform was evaluated. 100-fold diluted egg white and meat paste, and 10-fold diluted raw milk with the addition of *S. aureus* (0, 100 and 10000 CFU/mL) were analyzed. Satisfactory recoveries were obtained between 96.0% and 106.0% with relative standard deviations of 1.5% to 4.7% (Table S3). These results suggested that the proposed biosensor has potential application for real sample detection. Besides, the fabrication reproducibility of the sensing system was also examined by using ten sensors prepared independently. Close FL/ECL responses were obtained with a variation coefficient of 4.7%, indicating a reliable fabrication technique. After the biosensor was stored for 14 days, the FL/ECL value could retain 96.8% of its original signal, indicating the satisfactory stability of the sensing system for long-term operation.

Table S3. Detection of *S. aureus* in various food samples.

Samples	Added (CFU/mL)	Measured (CFU/mL)	Recovery (%)	RSD (%, n=5)
Egg white 1	0	5	−	3.1
Egg white 2	100	106	106.0	4.3
Egg white 3	10000	9670	96.7	3.2
Meat paste 1	0	6	−	3.7
Meat paste 2	100	96	96.0	4.7
Meat paste 3	10000	10420	104.2	2.4
Raw milk 1	0	8	−	2.7
Raw milk 2	100	105	105.0	3.9
Raw milk 3	10000	9720	97.2	1.5

Author contribution statement

Qiumei Feng: Conceptualization, Project administration, Validation, Writing - original draft. Tao Wu: Data curation, Methodology. Huan Wang: Formal analysis. Meisheng Wu: Data curation, Conceptualization, Writing - review & editing. Baoting Dou: Validation. Po Wang: Supervision, Funding acquisition, Conceptualization, Writing - review & editing.

References

S1 H. Zhou, J. Liu, J. Xu, H. Chen, *Chem. Commun.*, 2011, **47**, 8358.

S2 Y. Zhang, H. Zhou, P. Wu, H. Zhang, J. Xu, H. Chen, *Anal. Chem.*, 2014, **86**, 8657.

S3 S. Liu, Q. Li, H. Yang, P. Wang, X. Miao and Q. Feng, *Biosens. Bioelectron.*, 2022, **196**, 113744.

S4 K. Yuan, Q. Mei, X. Guo, Y. Xu, D. Yang, B. J. Sanchez, B. Sheng, C. Liu, Z. Hu, G. Yu, H. Ma, H. Gao, C. Haisch, R. Niessner, Z. Jiang and H. Zhou, *Chem. Sci.*, 2018, **9**, 8781.

S5 S. Zhou, C. Lu, Y. Li, L. Xue, C. Zhao, G. Tian, Y. Bao, L. Tang, J. Lin and J. Zheng, *ACS Sens.*, 2020, **5**, 588.

S6 Y. Lou, Q. Jia, F. Rong, S. Zhang, Z. Zhang and M. Du, *Food Chem.*, 2022, **395**, 133618.

S7 X. Sun, Y. Wang, L. Zhang, S. Liu, M. Zhang, J. Wang, B. Ning, Y. Peng, J. He, Y. Hu and Z. Gao, *Anal. Chem.*, 2020, **92**, 3032.

S8 Q. Ouyang, M. Zhang, Y. Yang, Z. Din and Q. Chen, *Food Control,* 2022, **145**, 109444.

S9 S. Zhan, H. Fang, J. Fu, W. Lai, Y. Leng, X. Huang and Y. Xiong, *J. Agr. Food Chem.*, 2019, **67**, 9104.

S10 Q. Li, M. Zhang, Q. Zhang, Z. Zhu, Z. Guo, J. Li, W. Xu, J. Zhu, Y. Yao and Z. Li, *Talanta*, 2023, **252**, 123833.

S11 S. Bu, X. Liu, Z. Wang, H. Wei, S. Yu, Z. Li, Z. Hao, W. Liu and J. Wan, *Sens. Actuators B-Chem.*, 2021, **347**, 130630.